

# Universal Density of Low Frequency States in Silica Glass at Finite Temperatures

Silvia Bonfanti<sup>1</sup>, Roberto Guerra<sup>1</sup>, Itamar Procaccia<sup>2,3</sup> and Stefano Zapperi<sup>1,4</sup>

<sup>1</sup>Center for Complexity and Biosystems, Department of Physics,  
University of Milan, via Celoria 16, 20133 Milano, Italy

<sup>2</sup> Dept. of Chemical Physics, The Weizmann Institute of Science, Rehovot 76100, Israel

<sup>3</sup>Center for OPTical IMagery Analysis and Learning,  
Northwestern Polytechnical University, Xi'an, 710072 China

<sup>4</sup> CNR - Consiglio Nazionale delle Ricerche, Istituto di Chimica della Materia  
Condensata e di Tecnologie per l'Energia, Via R. Cozzi 53, 20125 Milano, Italy

(Dated: September 21, 2021)

The theoretical understanding of the low-frequency modes in amorphous solids at finite temperature is still incomplete. The study of the relevant modes is obscured by the dressing of inter-particle forces by collision-induced momentum transfer that is unavoidable at finite temperatures. Recently, it was proposed that low frequency modes of vibrations around the *thermally averaged* configurations deserve special attention. In simple model glasses with bare binary interactions, these included quasi-localized modes whose density of states appears to be universal, depending on the frequencies as  $D(\omega) \sim \omega^4$ , in agreement with the similar law that is obtained with bare forces at zero temperature. In this Letter, we report investigations of a model of silica glass at finite temperature; here the bare forces include binary and ternary interactions. Nevertheless we can establish the validity of the universal law of the density of quasi-localized modes also in this richer and more realistic model glass.

**Introduction:** Simple models of amorphous solids employ ensembles of particles interacting via binary forces [1]. Choosing different sizes of particles (or equivalently, ranges of interaction of these forces), one can create useful models of glass forming systems. In athermal conditions ( $T=0$ ), these given forces offer also a straightforward path to analyzing the vibrational modes around a local energy minimum state [2]. The bare Hamiltonian  $U(\mathbf{r}_1, \dots, \mathbf{r}_N)$  provides the Hessian matrix  $\mathbf{H}$  which determines, in the harmonic approximation, all the modes and their frequencies [3]

$$H_{ij}^{\alpha\beta} \equiv \frac{\partial^2 U(\mathbf{r}_1, \dots, \mathbf{r}_N)}{\partial r_i^\alpha \partial r_j^\beta}. \quad (1)$$

Here  $\mathbf{r}_i$  is the  $i$ th coordinate of a constituent particle in a system with  $N$  particles. As long as the  $T=0$  configuration is stable, all the eigenvalues of the bare Hessian are real and positive (with the exception of few possible zeros associated with Goldstone modes). The force on each particles  $\mathbf{F}_i$  is given by  $-\partial U(\mathbf{r}_1, \dots, \mathbf{r}_N)/\partial \mathbf{r}_i$  and it vanishes for all  $i$ 's in athermal equilibrium. One then computes the eigenfunctions and eigenvalues of the Hessian  $\mathbf{H}$ . The eigenvalues  $\lambda_i$  are related to the frequency  $\omega_i$  according to

$$\omega_i = \pm \sqrt{\lambda_i}. \quad (2)$$

In amorphous solids, the eigenfunctions can be extended or quasi-localized, with possible hybridization between these classes. In principle, one can distinguish between these different types of modes by considering the participation ratio  $PR$  which is defined as in previous papers [4]

$$PR = [N \sum_i (\mathbf{e}_i \cdot \mathbf{e}_i)^2]^{-1}, \quad (3)$$

where  $\mathbf{e}_i$  is the  $i$ th element of a given eigenfunction of the Hessian matrix. We expect the participation ratio to be of order  $O(1/N)$  for a quasi-localized mode (QLM) and of order unity for an extended mode. It was expected for a long time [5–8] that the QLM's display a density of states  $D(\omega)$  with a universal power law

$$D(\omega) \sim \omega^4 \quad \text{in all dimensions.} \quad (4)$$

The actual verification of this prediction was, however, slow in coming. The difficulty is that in large systems the QLM's hybridize strongly with low frequency delocalized elastic extended modes. The latter are expected to follow the Debye theory, with density of states depending on frequency as  $\omega^{d-1}$  where  $d$  is the spatial dimension. Recently, a remedy was found: By examining *small* systems one can bound the frequency of Debye modes from below, exposing the low-frequency QLM's to shine in isolation [9]. Indeed, in such circumstances the universal law Eq. (4) can easily be demonstrated. A direct verification of such a law with numerical simulations of glass formers with binary interactions [10–15] and for silica glass with binary and ternary interactions [4, 16] was recently achieved.

Once we turn to finite temperatures, however, it is not immediately obvious how to examine the existence of a similar universal law. The system is never at rest, with particles moving, colliding, and imparting momentum. The bare Hessian matrix Eq. (1) loses its usefulness, since it generically gains negative eigenvalues when computed in a given frozen configuration. The total force  $\mathbf{F}_i$  on an  $i$ th particle, as computed from the bare Hamiltonian, does not vanish, and the eigenfunctions of the bare Hessian lose their meaning as modes associated with a frequency of vibration around a well defined energy min-

imum. We thus need a new definition of modes that mimics their athermal counterparts.

A recently proposed idea focuses on the thermal *average* positions of our particles, and the modes of fluctuations around these [17, 18]. The average positions of a thermal glass are constant on time scales shorter than the typical diffusion time  $\tau_G$ . We thus need to consider relatively stable glasses at sufficiently low temperatures such that the cage structure around every particle remains stable, apart from thermal motion, for times that are sufficiently long to allow the evaluation of the average position of each particle, but sufficiently shorter than the diffusion time at which the cage structure is destroyed. At these average positions, the bare forces do not vanish, but one can consider effective forces which are derived from an effective Hamiltonian that takes into account the dressing of the forces due to the momentum transfer during collisions. Of course, these forces will no longer be binary, but rather have ternary, quaternary and higher order contributions [19, 20]. While it is quite hard to determine precisely the effective forces, it is rather straightforward to define the effective Hessian. To this end, we compute the time averaged positions  $\mathbf{R}_i$ :

$$\mathbf{R}_i \equiv \frac{1}{\tau} \int_0^\tau dt \mathbf{r}_i(t), \quad (5)$$

where  $\tau \ll \tau_G$ . By definition, the positions  $\mathbf{R}_i$  are time independent and the configuration  $\{\mathbf{R}_i\}_{i=1}^N$  is stable, at least within the time interval  $[0, \tau_G]$ . An additional quantity of importance is the covariance matrix  $\mathbf{\Sigma}$ , defined as

$$\Sigma_{ij} \equiv \frac{1}{\tau} \int_0^\tau dt (\mathbf{r}_i(t) - \mathbf{R}_i) (\mathbf{r}_j(t) - \mathbf{R}_j). \quad (6)$$

We can now define an effective Hessian via

$$\mathbf{H}^{(\text{eff})} = k_B T \mathbf{\Sigma}^+. \quad (7)$$

Here  $\mathbf{\Sigma}^+$  is the pseudo-inverse of the covariance matrix. Next, we note that the effective Hessian given by Eq. (7) and the covariance matrix have the same set of eigenfunctions

$$\mathbf{H}^{(\text{eff})} \mathbf{\Psi}_i = \lambda_i^H \mathbf{\Psi}_i \quad (8)$$

and their eigenvalues are related by

$$\lambda_i^H = \frac{k_B T}{\lambda_i^{\Sigma^+}}. \quad (9)$$

In Ref. [17], it was shown that the eigenvalues and eigenfunctions of  $\mathbf{H}^{(\text{eff})}$  serve the same role for the time-averaged configuration as the corresponding ones for the bare Hessian play for the athermal configuration. Indeed, in simple model glass formers one could show that the QLM's of  $\mathbf{H}^{(\text{eff})}$  have a universal density of states of the form of Eq. (4). The aim of this paper is to examine

how universal this result is by studying in silica glass at non vanishing temperatures.

**The model silica glass** The silica glass is simulated in a 3-dimensional cubic box for two different system sizes:

- $N = 1032$  atoms, therefore  $N_{Si} = 344$  silicon atoms and  $N_O = 688$  oxygen atoms, with a box length  $L = 25 \text{ \AA}$
- $N = 4008$  atoms, therefore  $N_{Si} = 1336$  silicon atoms and  $N_O = 2672$  oxygen atoms with a box length  $L = 39.3 \text{ \AA}$ ,

The interaction between atoms is given by the Vashishta's potential [21]. In this paper, units are defined on the basis of energy, length, and time, respectively being eV,  $\text{\AA}$ , and ps.

*Preparation Protocol.* Following Ref. [22], glass samples are initially prepared with randomly positioned Si,O atoms with a density  $\rho_{in} = 2.196 \text{ g/cm}^3$  and an annealing protocol: (i) 2 ps of Newtonian dynamics where atoms have Lennard-Jones interactions and are viscously damped with a rate of 1/ps and atomic velocities limited to 1  $\text{\AA}$ /ps, (ii) 8 ps of damped Newtonian dynamics with Vashishta's potential for silica glass. (iii) Heating up the system up to 4000 K and then quench to 0 K in 100 ps, corresponding to a cooling rate of 40 K/ps. The so-produced configurations are then minimized through the fast inertial relaxation engine (FIRE) [23] until the total force on every atom satisfies  $|\mathbf{F}_i| \leq 10^{-10} \text{ eV/\AA}$ .

*Simulations at non-vanishing temperatures.* We perform simulations using a Langevin thermostat (damping parameter 1 ps) at  $T = 1, 2, 4, 8 \text{ K}$  for 50 ps followed by NVE ensemble simulations for 100 ps (200 ps) for the smallest (largest) system size, monitoring the mean square displacements (MSD) of the atoms. The total number of starting configurations for each temperature is 1000. Differently from our previous works on silica glasses [24, 25] where we used a different interatomic potential, we use here the Vashishta's potential as implemented in LAMMPS [26] since it is more efficient in terms of computation time.

**Results:** To guarantee that our measurements do not exceed the time window in which diffusion does not play a role, we measure the Mean-Square-Displacement (MSD) of our particles at each temperature  $T$ . Since the covariance matrix Eq. (6) has to be measured inside the glass basin, we must insure that the system is still in the basin prepared at  $t=0$ . Figure 1 presents the MSD as a function of time. Obviously, when the temperature is too high, the system escapes from the basin, preventing us from measuring a stationary covariance matrix. On the other hand for low temperatures (from  $T=1 \text{ K}$  up to  $T=32 \text{ K}$ ), the MSD reaches a plateau which survives throughout our simulation window (1000 ps). Note that as the temperature increases, so the plateau increases, as expected from solid mechanics. At a finite

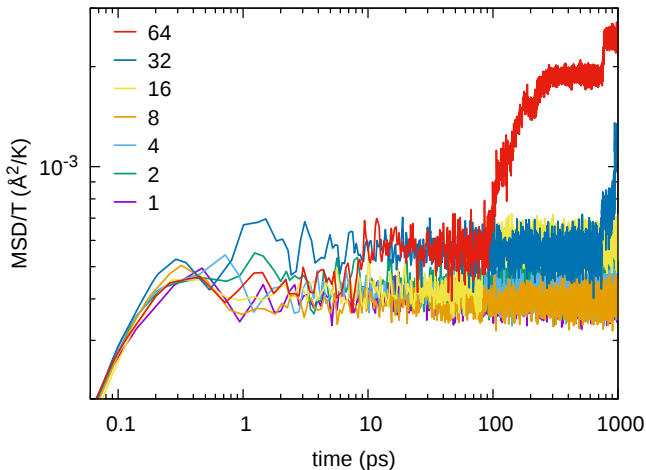


FIG. 1. Starting from the inherent structure configuration, we perform MD monitoring the mean squared displacement. Here we plot MSD vs. time. In the considered time window, at a large-enough  $T$  the cages break and the MSD deviates from the plateau. From the Figure we obtain that up to  $T=8$  K no diffusion is observed within the 1 ns timeframe.

temperature-dependent timescale  $\tau_G$  the MSD departs from the plateau, meaning that diffusion sets in and the system departs from the local minimum. In practice, we have to compute the covariance matrix within the range of the plateau, before the MSD displays the upturn.

We show the density of states obtained by the covariance matrix at finite temperatures (from 1 K to 8 K) in Figure 2. Panels (a) and (c) show the density of states including all modes for the two system sizes and the dashed line correspond to the  $\omega^4$  scaling law. Only at very low frequency, the DOS appears to obey the  $\omega^4$  scaling; for  $N=1032$  the behavior is observed in a very short range of frequencies, but for the bigger sample  $N=4008$  this trend is clearer. To exhibit the scaling law more convincingly, we need to select only QLM's. To this end, we include only the modes having participation ratio below 0.1. Indeed after these modes are selected, we see in panels (b) and (d) that the DOS obeys clearly the  $\omega^4$  scaling. We note that in the case of the small system of 1032 particles (Fig. 2 (b) at very low  $\omega$ , the DOS is much smaller than the expected  $\omega^4$  scaling; this is possibly due to finite size effects. Indeed in the larger samples of 4008 particles in panel (d), the DOS shows  $\omega^4$  scaling down to very lowest available frequencies. According to Figure 2, our data show the  $\omega^4$  scaling also in the finite temperature regime for the realistic silica glass model. Together with the previously investigated simple binary mixture systems [18], this implies that the  $\omega^4$  scaling law is robust and universal, existing in different glass models also at finite temperature.

It is interesting to note that recent analysis led two groups to present density of states with power laws fol-

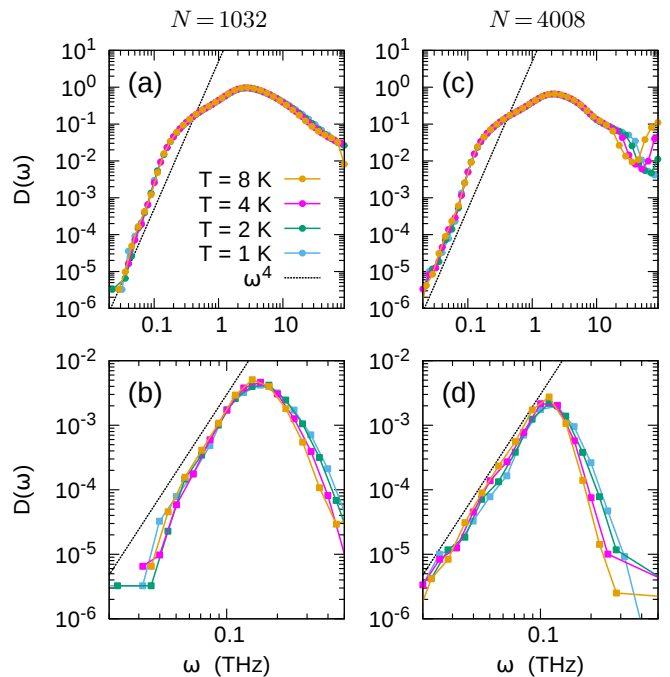


FIG. 2. Density of states as computed from the effective Hessian at different temperatures,  $T=1, 2, 4, 8$  K, for SiO<sub>2</sub> glass samples of 1032 (panels (a) and (b)) and 4008 (panels (c) and (d)) atoms. In panels (a) and (c) all the eigenfrequencies are included whereas in panels (b) and (d) only the modes with participation ratio smaller than 0.1 are considered. For all  $T$  values, data from over 1000 samples was included.

lowing  $\omega^3$  [27] and  $\omega^5$  [28] respectively. Having in mind that in the present case the scaling range of the  $\omega^4$  scaling law is rather limited, we turn now to extreme value statistics to lend further support to the  $\omega^4$  law. Since we have many configurations in our simulations, we can determine the minimal frequency obtained from the diagonalization of  $\mathbf{H}^{(\text{eff})}$  in each and every configuration, denoting it as  $\omega_{\min}$ . The average of this minimal frequency over the ensemble of configurations is  $\langle \omega_{\min} \rangle$ . Referring to the argument first presented in Ref. 29, we expect that in systems with  $N$  particles,

$$\int_0^{\langle \omega_{\min} \rangle} D(\omega) d\omega \sim N^{-1}. \quad (10)$$

Using Eq. (4), we then expect that in three dimensions

$$\langle \omega_{\min} \rangle \sim N^{-1/5} \sim L^{-3/5}. \quad (11)$$

Moreover, since the different realization are uncorrelated, the values of  $\omega_{\min}$  are also uncorrelated. Then the well-known Weibull theorem [30] predicts that the distribution of  $\omega_{\min}$  should obey the Weibull distribution in the limit of large  $N$

$$W(\omega_{\min}) = \frac{5(\Gamma(1.2))^5}{\langle \omega_{\min} \rangle^5} \omega_{\min}^4 e^{-\left(\frac{\omega_{\min} \Gamma(1.2)}{\langle \omega_{\min} \rangle}\right)^5}, \quad (12)$$

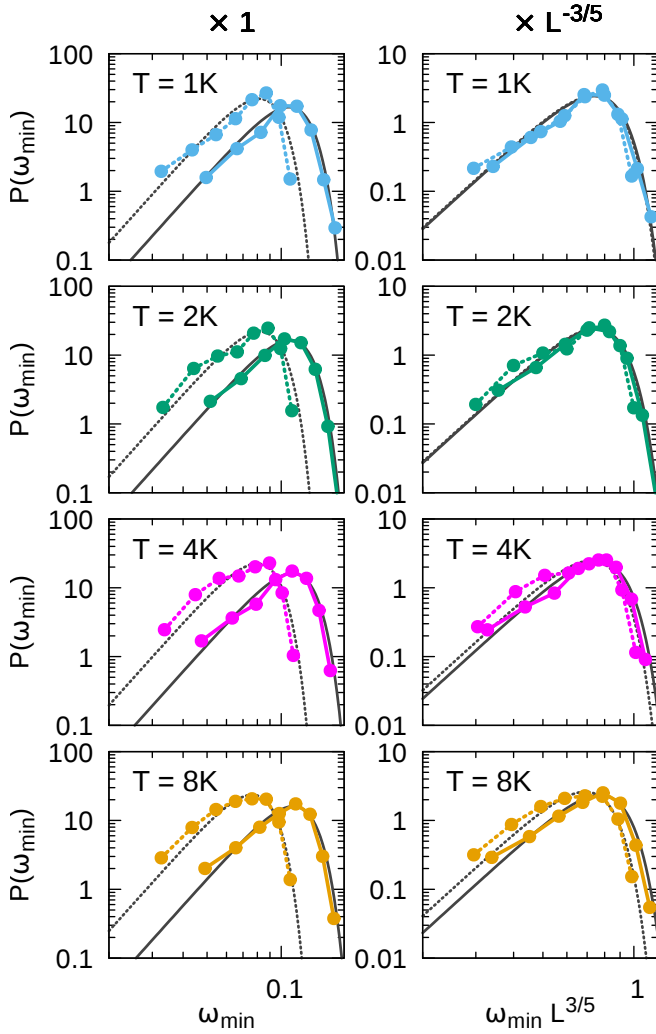


FIG. 3. Left panels: Distribution of the minimal vibrational frequency  $P(\omega_{\min})$  for the two investigated system sizes ( $N = 1032$  solid lines and symbols,  $N = 4008$  dotted lines and symbols) and four temperatures  $T$ . The gray lines are the corresponding Weibull distributions, Eq. 12. Right panels: Rescaled distributions according to Eq. (11).

where  $\Gamma(x)$  is the Gamma function,  $\Gamma(1.2) \approx 0.918$ . This prediction is tested in four left panels of Fig. 3. The distributions of  $\omega_{\min}$  for the two system sizes and four values of the temperature  $T$  are shown, together with the fitted distribution Eq. (12). Finally, the scaling shown by Eq. (11) indicates that the distributions can be collapsed by plotting them as a function of the rescaled minimal frequency  $\omega_{\min} L^{3/5}$ . The rescaling of the curves by  $L^{3/5}$  is reported in the right panels of Fig. 3. The data collapse is very good with slight deviations starting at  $T = 8K$ . We reiterate that this is a strong independent test of Eq. (4).

**Summary and Conclusions:** The main aim of this Letter was to examine whether the universality class that is expressed by Eq. (4) extends to finite temperatures in

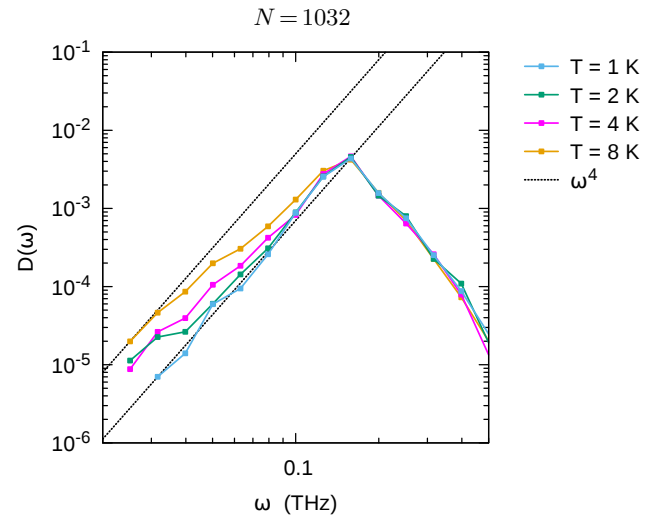


FIG. 4. Density of states as computed from the standard Hessian at different temperatures,  $T = 1, 2, 4, 8$  K, for  $\text{SiO}_2$  glass samples of 1032 particles. Only the modes with participation ratio smaller than 0.1 are considered. For all  $T$  value, statistics over 1000 samples was accounted.

glasses whose interactions are richer than those of simple glass formers with binary interactions [18]. One needs to understand that the bare Hessian, which can be computed for a frozen configuration, does not yield a scaling law of this form. Firstly, generically its diagonalization yields negative eigenvalues (i.e imaginary frequencies), since any arrested state is unstable. However, when computed over the  $\mathbf{R}_i$  coordinates, Eq. 5, it turns out that in the present case of silica glass, most of the configurations do not have negative eigenvalues, while the number of the latter tend to increase with  $T$ . Therefore, one can consider the density of states, excluding configurations with negative eigenvalues. Selecting these modes, and filtering according to the same criterion, i.e. including only modes whose participation ratio is smaller than 0.1, we obtain the density of states shown in Fig. 4. The distribution resembles the unfiltered probability density functions in panels (a) and (c) of Fig. 2. Only by computing  $\mathbf{H}^{(\text{eff})}$  and filtering out the modes with high participation ratio do we get probability density functions that correspond to the scaling law (4)

**Acknowledgments** – R.G. acknowledges financial support from Università degli Studi di Milano, grant no. 1094 SEED 2020 - TEQUAD. The work of I.P. was supported in part by the US-Israel Binational Science Foundation and the Minerva Foundation, Munich, Germany.

[1] Walter Kob and Hans C. Andersen. Kinetic lattice-gas model of cage effects in high-density liquids and a test of

- mode-coupling theory of the ideal-glass transition. *Phys. Rev. E*, 48:4364–4377, Dec 1993.
- [2] D. L. Malandro and D. J. Lacks. *The Journal of Chemical Physics*, 110(9):4593–4601, 1999.
- [3] C. E. Maloney and A. Lemaître. *Physical Review E*, 74(1):016118, 2006.
- [4] Silvia Bonfanti, Roberto Guerra, Chandana Mondal, Itamar Procaccia, and Stefano Zapperi. Universal low-frequency vibrational modes in silica glasses. *Phys. Rev. Lett.*, 125:085501, Aug 2020.
- [5] U. Buchenau, Yu. M. Galperin, V. L. Gurevich, and H. R. Schober. *Phys. Rev. B*, 43:5039–5045, 1991.
- [6] V. Gurarie and J. T. Chalker. *Phys. Rev. B*, 68:134207, 2003.
- [7] V. L. Gurevich, D. A. Parshin, and H. R. Schober. *Phys. Rev. B*, 67:094203, 2003.
- [8] D. A. Parshin, H. R. Schober, and V. L. Gurevich. *Phys. Rev. B*, 76:064206, 2007.
- [9] E. Lerner, G. Düring, and E. Bouchbinder. *Phys. Rev. Lett.*, 117:035501, 2016.
- [10] M. Baity-Jesi, V. Martín-Mayor, G. Parisi, and S. Perez-Gaviro. *Phys. Rev. Lett.*, 115:267205, 2015.
- [11] L. Angelani, M. Paoluzzi, G. Parisi, and G. Ruocco. *PNAS*, 115:8700–8704, 2018.
- [12] M. Shimada, H. Mizuno, M. Wyart, and A. Ikeda. *Phys. Rev. E*, 98:060901, 2018.
- [13] H. Mizuno, H. Shiba, and A. Ikeda. *PNAS*, 114:E9767–E9774, 2017.
- [14] G. Kapteijns, E. Bouchbinder, and E. Lerner. *Phys. Rev. Lett.*, 121:055501, 2018.
- [15] A. Moriel, G. Kapteijns, C. Rainone, J. Zylberg, E. Lerner, and E. Bouchbinder. *J. Chem. Phys.*, 151:104503, 2019.
- [16] K. Gonzalez Lopez, D. Richard, G. Kapteijns, R. Pater, T. Vaknin, E. Bouchbinder, and E. Lerner. *arXiv:2003.07616*, 2020.
- [17] P. Das, V. Ilyin, and I. Procaccia. Instabilities of time-averaged configurations in thermal glasses. *Phys. Rev. E*, 100:062103, 2019.
- [18] Prasenjit Das and Itamar Procaccia. Universal density of low-frequency states in amorphous solids at finite temperatures. *Physical Review Letters*, 126(8):085502, 2021.
- [19] Oleg Gendelman, Edan Lerner, Yoav G. Pollack, Itamar Procaccia, Corrado Rainone, and Birte Riechers. Emergent interparticle interactions in thermal amorphous solids. *Phys. Rev. E*, 94:051001, Nov 2016.
- [20] Giorgio Parisi, Itamar Procaccia, Carmel Shor, and Jacques Zylberg. Effective forces in thermal amorphous solids with generic interactions. *Physical Review E*, 99(1):011001, 2019.
- [21] Jeremy Q Broughton, Christopher A Meli, Priya Vashishta, and Rajiv K Kalia. Direct atomistic simulation of quartz crystal oscillators: Bulk properties and nanoscale devices. *Physical Review B*, 56(2):611, 1997.
- [22] Silvia Bonfanti, Roberto Guerra, Chandana Mondal, Itamar Procaccia, and Stefano Zapperi. Universal low-frequency vibrational modes in silica glasses. *Physical Review Letters*, 125(8):085501, 2020.
- [23] Erik Bitzek, Pekka Koskinen, Franz Gähler, Michael Moseler, and Peter Gumbsch. Structural relaxation made simple. *Physical review letters*, 97(17):170201, 2006.
- [24] S. Bonfanti, Ezequiel E. Ferrero, Alessandro L. Sellario, Roberto Guerra, and Stefano Zapperi. Damage accumulation in silica glass nanofibers. *Nano Letters*, 18(7):4100–4106, 2018. PMID: 29856226.
- [25] S. Bonfanti, R. Guerra, C. Mondal, I. Procaccia, and S. Zapperi. Elementary plastic events in amorphous silica. *Phys. Rev. E*, 100:060602, Dec 2019.
- [26] S. Plimpton, P. Crozier, and A. Thompson. Lammpl-large-scale atomic/molecular massively parallel simulator. *Sandia National Laboratories*, 18:43, 2007.
- [27] Lijin Wang, Grzegorz Szamel, and Elijah Flenner. Low-frequency excess vibrational modes in two-dimensional glasses, 2021.
- [28] Vishnu V. Krishnan, Kabir Ramola, and Smarajit Karmakar. Universal non-debye low-frequency vibrations in sheared amorphous solids, 2021.
- [29] S. Karmakar, E. Lerner, and I. Procaccia. *Phys. Rev. E*, 82:055103, 2010.
- [30] W. Weibull. *A Statistical Theory of the Strength of Materials*. Generalstabens litografiska anstalts förlag, Stockholm, 1939.